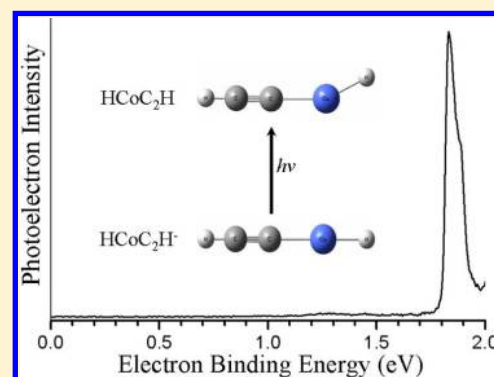


Photoelectron Spectroscopy of CoC_2H_2^- and Density Functional Study of $\text{Co}_n\text{C}_2\text{H}_2$ ($n = 1-3$) Anion and Neutral Clusters

Jinyun Yuan,[†] Gao-Lei Hou,[‡] Baocheng Yang,[†] Hong-Guang Xu,[‡] and Wei-Jun Zheng^{*‡}[†]Institute of Nanostructured Functional Materials, Huanghe Science and Technology College, Zhengzhou, Henan 450006, China[‡]Beijing National Laboratory for Molecular Sciences, State Key Laboratory of Molecular Reaction Dynamics, Institute of Chemistry, Chinese Academy of Sciences, Beijing 100190, China

Supporting Information

ABSTRACT: The anionic and neutral $\text{Co}_n\text{C}_2\text{H}_2$ ($n = 1-3$) clusters were investigated using anion photoelectron spectroscopy and density functional calculations. The adiabatic detachment energies and vertical detachment energies of $\text{Co}_n\text{C}_2\text{H}_2^-$ ($n = 1-3$) were determined. Our results show that the most stable geometries of anionic $\text{Co}_n\text{C}_2\text{H}_2^-$ ($n = 1-2$) and neutral $\text{Co}_n\text{C}_2\text{H}_2$ ($n = 1-3$) are composed of $\text{Co}_n\text{C}_2\text{H}$ clusters adsorbing a hydrogen atom on the top or bridge sites of Co_n , whereas $\text{Co}_3\text{C}_2\text{H}_2^-$ consists of a five-member ring of Co_3C_2 carbide adsorbing two hydrogen atoms on two bridge sites of Co_3 . The reaction mechanisms show that the inserted isomer HCoC_2H can convert into the vinylidene complex $\text{Co}=\text{C}=\text{CH}_2$ via a side-on isomer $\text{M}-\eta^2-(\text{C}_2\text{H}_2)$.



1. INTRODUCTION

The reactions of hydrocarbons on transition metals are one of the most important industrial catalytic processes. Therefore, the interactions of transition metals with the typical and simplest unsaturated hydrocarbons like acetylene have received considerable attention from both experimental and theoretical points of view. Four kinds of transition metal–acetylene complexes have been addressed via the reactions of transition metals with acetylene, including the side-on $\text{M}-(\eta^2-\text{C}_2\text{H}_2)$, the vinyl $\text{M}-\text{C}_2\text{H}_2$, the inserted $\text{HM}-\text{CCH}$, and the vinylidene $\text{M}=\text{C}=\text{CH}_2$.¹⁻¹⁶ Zhou and co-workers found that the ground-state Cr atoms reacted with acetylene to form metal-cyclopropene, which will rearrange into the inserted product upon ultraviolet–visible irradiation.⁹ Recently, using matrix isolation infrared spectroscopy and density functional theory (DFT) calculations, Andrews and co-workers have reported that the reactions of laser-ablated transition metals (Sc, Y, La, Cr, Mo, W) with acetylene produce the π and the inserted complexes.^{13,16} Xu and co-workers have identified the products of the side-on $\text{M}-(\eta^2-\text{C}_2\text{H}_2)$ ($\text{M} = \text{Y}, \text{Ge}, \text{Sn}$), the inserted HYCCH ($\text{M} = \text{Y}, \text{Ge}, \text{Sn}, \text{Pb}$), anionic HScCCH^- , HScScCCH^- , and the vinylidene $\text{Sn}_2\text{C}=\text{CH}_2$.^{7,17} Duncan and co-workers investigated the cationic $\text{M}^+(\text{C}_2\text{H}_2)$ complexes ($\text{M} = \text{Ca}, \text{V}, \text{Fe}, \text{Co}, \text{and Ni}$) by using infrared photodissociation spectroscopy and theoretical calculations.¹⁸⁻²¹ Ramsvik et al. studied the chemisorption and decomposition of acetylene on the Co single-crystal surface using the near-edge X-ray absorption fine structure (NEXAFS) technique²² and observed that the dehydrogenated fragment C_2H was adsorbed on the Co crystal surface in the temperature range of 200–300 K.

Although many investigations on the interactions of metals with acetylene have been carried out, the interactions between anionic/neutral cobalt clusters and acetylene have not been studied. Cobalt is an effective and inexpensive catalyst in the field of chemical industry. For example, cobalt catalysts have been used for Fisher–Tropsch (hydrocarbon) synthesis in the industry²³ and are applicable for C–C bond formations.^{24,25} The study of $\text{Co}_n\text{C}_2\text{H}_2$ ($n = 1-3$) clusters may provide insights into the heterogeneous hydrocarbon catalysis at the molecular level. In this work, we investigated anionic and neutral $\text{Co}_n\text{C}_2\text{H}_2$ ($n = 1-3$) clusters using anion photoelectron spectroscopy and DFT calculations.

2. EXPERIMENTAL AND THEORETICAL METHODS

The experiments were conducted on a home-built apparatus consisting of a time-of-flight mass spectrometer and a magnetic bottle photoelectron spectrometer, which has been described elsewhere.²⁶ The anionic CoC_2H_2^- cluster was generated in a laser vaporization source in which a rotating and translating cobalt target was ablated with the second harmonic light (532 nm) of a Nd:YAG laser (Continuum Surelite II–10) while helium gas with ~ 4 atm backing pressure seeded with ethene molecules ($\sim 2\%$) was allowed to expand through a pulsed valve over the cobalt target. The anionic CoC_2H_2^- cluster was mass-selected and decelerated before being photodetached using the second (532 nm) and the fourth (266 nm) harmonic lights of a

Received: May 19, 2014

Revised: July 30, 2014

Published: July 30, 2014

second Nd:YAG laser, respectively. The photodetached electrons were energy-analyzed by the magnetic bottle photoelectron spectrometer. The photoelectron spectra were calibrated using the spectra of Cu^- taken at similar conditions. The energy resolution of the photoelectron spectrometer was approximately 40 meV for the electrons of 1 eV kinetic energy.

DFT calculations with the B3LYP^{27–30} exchange–correlation potential and 6-311++G(d,p) basis set were carried out to obtain the structures of anionic and neutral $\text{Co}_n\text{C}_2\text{H}_2$ ($n = 1–3$) clusters. The B3LYP functional has been widely used for organic transition-metal compounds.^{1,13,14,31} Many density functionals can be employed to study the complexes involving transition metals, which have been discussed in details in a number of references.^{32–34} In this work, we tested several functionals such as B3LYP, BPW91, and BP86 for the $\text{Co}_n\text{C}_2\text{H}_2$ ($n = 1–3$) system (Table S1, Supporting Information). We found that the VDE of CoC_2H_2^- calculated with the B3LYP functional is in better agreement with the experimental measurement. Thus, we used the B3LYP functional for all calculations in this work. To test the influence of basis sets on the bond lengths and energies, calculations of the CoC_2H_2^- cluster were also carried out using the Def2-QZVPD basis set. The results (Table S2, Supporting Information) show that the relative energies, vertical detachment energies (VDEs), and C–C bond lengths from the 6-311++G(d,p) and Def2-QZVPD basis sets are very close to each other. However, the Def2-QZVPD basis set is more expensive than the 6-311++G(d,p) basis set. Thus, we used the 6-311++G(d,p) basis set in this work.

Conversion mechanisms among the isomers of the neutral CoC_2H_2 cluster were also calculated. Geometry optimizations were conducted without any symmetry constraint. Vibrational frequencies were calculated to ensure that all of the optimized isomers are real minima and each transition-state structure has a unique imaginary frequency. Intrinsic reaction coordinate (IRC) calculations were carried out to confirm the transition states connecting the desired reactants and the products.^{35,36} The theoretical VDEs were calculated as the energy differences between the neutrals and anions both at the geometries of the anionic species. The theoretical adiabatic detachment energies (ADEs) were calculated as the energy differences between the neutrals and the anions with the neutral structures relaxed to the nearest local minima using the geometries of the corresponding anions as initial structures. For the anionic clusters with multiplicity M , the neutral species with multiplicities $M - 1$ and $M + 1$ were considered in the VDE and ADE calculations. All energies were corrected by zero-point vibrational energies. The spin multiplicities and spin contaminations were also considered in the calculations. The calculations were performed with the GAUSSIAN03 program package.³⁷

3. EXPERIMENTAL RESULTS

The photoelectron spectra of CoC_2H_2^- measured with 532 and 266 nm photons are shown in Figure 1. At 266 nm, the photoelectron spectrum of CoC_2H_2^- has three well-resolved features centered at 1.85, 2.0, and 2.26 eV, respectively. It also has an enhanced band feature at 3.53 eV. In the 532 nm spectrum, only one peak centered at 1.83 eV is observed. The VDE of CoC_2H_2^- was obtained from the maximum of the peak in the 532 nm spectrum, and thus, the VDE of CoC_2H_2^- is 1.83 eV. The ADE was determined by adding the value of the instrumental resolution to the onset of the peak of CoC_2H_2^- in

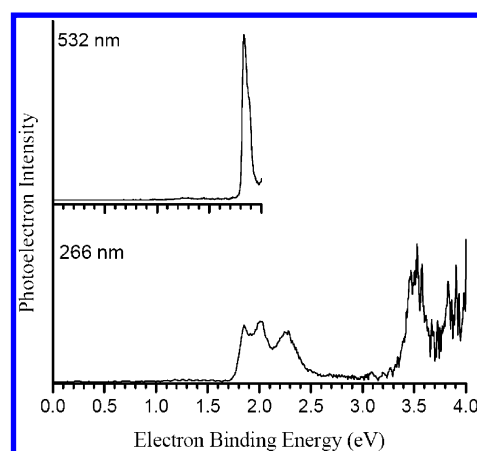


Figure 1. Photoelectron spectra of the anionic CoC_2H_2^- cluster recorded with 532 and 266 nm photons.

the 532 nm spectrum. The onset of the peak was determined by drawing a straight line along the leading edge of the first peak to cross the baseline of the spectrum. In this way, the ADE of CoC_2H_2^- was estimated to be 1.82 eV. On the basis of the difference between the peaks at 3.53 and 1.85 eV in the 266 nm photoelectron spectrum of CoC_2H_2^- , we suggest that an electronic excited state of neutral CoC_2H_2 ($\text{HCoC}=\text{CH}$) locates 1.68 eV above the ground state. It would be interesting if this transition could be confirmed using fluorescence or REMPI techniques by optical spectroscopy groups.

4. THEORETICAL RESULTS AND DISCUSSION

The geometries of the low-lying isomers of anionic and neutral $\text{Co}_n\text{C}_2\text{H}_2$ ($n = 1–3$) clusters obtained with DFT calculations are presented in Figures 2 and 3. In order to get the global

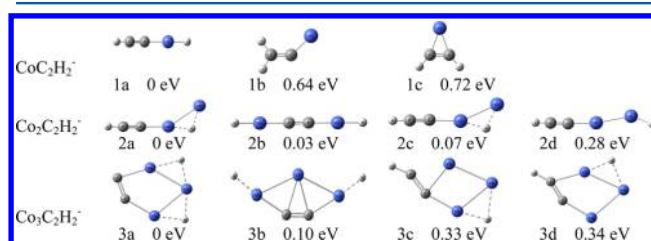


Figure 2. Geometries of the low-lying isomers of anionic $\text{Co}_n\text{C}_2\text{H}_2^-$ ($n = 1–3$).

minimum structure, we considered all possible spin multiplicities and various initial structures, such as the inserted

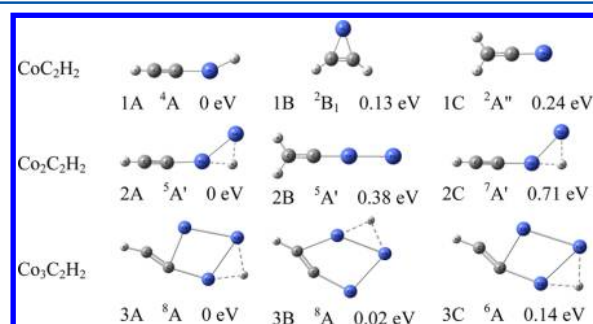


Figure 3. Geometries, relative energies, and electronic states of the low-lying isomers of neutral $\text{Co}_n\text{C}_2\text{H}_2$ ($n = 1–3$).

structures of Co atoms/clusters between two C atoms or between the C and H atoms of acetylene, the vinylidene structure Co_nCCH_2 , the side-on complex $\text{Co}_n\text{-}\eta^2\text{-(C}_2\text{H}_2)$, and the structures of cobalt carbides adsorbing a hydrogen molecule dissociatively/associatively. In order to calculate the ADEs of anionic clusters, the structures of neutral $\text{Co}_n\text{C}_2\text{H}_2$ ($n = 1\text{--}3$) clusters were also optimized using the anionic structures as initial structures. The calculated relative energies (ΔE), VDEs, and ADEs of anionic $\text{Co}_n\text{C}_2\text{H}_2^-$ ($n = 1\text{--}3$) clusters are listed in Table 1, in which the experimental values of CoC_2H_2^- are also presented for comparison. The bond lengths calculated at the B3LYP level will also be discussed in the following paragraphs.

Table 1. Relative Energies (ΔE) of the Low-Lying Isomers for $\text{Co}_n\text{C}_2\text{H}_2^-$ ($n = 1\text{--}3$) Clusters as Well as Their Theoretical and Experimental VDEs and ADEs

isomer	state	ΔE (eV)	VDE (eV)		ADE (eV)		
			theo.	expt.	theo.	expt.	
CoC_2H_2^-	1a	$^3\Sigma$	0	1.97	1.83	1.96	1.82
	1b	$^3A''$	0.64	1.22		0.83	
	1c	5A_2	0.72	1.05		0.81	
$\text{Co}_2\text{C}_2\text{H}_2^-$	2a	$^6A'$	0	1.80		1.57	
	2b	6A	0.03	3.41		3.35	
	2c	$^4A''$	0.07	1.53		1.49	
	2d	$^6A'$	0.28	2.53		1.28	
$\text{Co}_3\text{C}_2\text{H}_2^-$	3a	7A	0	2.34		2.27	
	3b	7A	0.10	3.10		2.16	
	3c	7A	0.33	1.42		1.42	
	3d	7A	0.34	1.69		1.59	

A. Anionic $\text{Co}_n\text{C}_2\text{H}_2^-$ ($n = 1\text{--}3$) Clusters. For CoC_2H_2^- , the most stable isomer (1a) is a linear configuration with the Co atom inserting into a C–H bond of free acetylene molecule. The C–C bond length of isomer 1a is calculated to be 1.23 Å, very close to the $\text{C}\equiv\text{C}$ bond of free acetylene (1.20 Å),³⁸ indicating that it is essentially a triple bond. The calculated Co–C bond length is 1.93 Å, only slightly longer than the covalent bond of Co–C (1.83 Å),³⁹ revealing a strong interaction between Co and C. The Co–H bond length is calculated to be 1.57 Å. The calculated ADE and VDE of isomer 1a are 1.96 and 1.97 eV, respectively, in reasonable agreement with the experimental values (1.82 and 1.83 eV). Isomer 1b is a vinylidene structure, and it is 0.64 eV higher in energy than isomer 1a. The theoretical VDE of isomer 1b (1.22 eV) is much lower than our experimental value (1.83 eV). Isomer 1c has a side-on $\text{Co-}\eta^2\text{-(C}_2\text{H}_2)$ structure and is 0.72 eV higher in energy than isomer 1a. The theoretical VDE (1.05 eV) of isomer 1c is also much lower than the experimental measurement (1.83 eV). Thus, isomer 1a is suggested to be the most probable structure produced in the experiments. We investigated the adsorption of the ethynyl radical (C_2H) on cobalt clusters before.⁴⁰ By comparing CoC_2H_2^- and CoC_2H^- , we found that CoC_2H_2^- may be formed by the linear CoC_2H^- adsorbing a hydrogen atom via the terminal cobalt. The CoC_2H^- adsorbing a hydrogen atom leads to a closed-shell structure, which may be the reason that the ADE of CoC_2H_2^- (1.82 eV) is much larger than that of CoC_2H^- (1.19 eV).

For $\text{Co}_2\text{C}_2\text{H}_2^-$, three nearly energetically degenerate isomers 2a, 2b, and 2c are found. The most stable isomer (2a) may be formed by the inserted HCoC_2H^- (isomer 1a) attaching a Co atom via the Co–Co bond. It can also be described as a

hydrogen atom adsorbed on the Co–Co bond of the $\text{Co}_2\text{C}_2\text{H}$. The C–C bond length is calculated to be 1.23 Å, identical to that of CoC_2H_2^- . The calculated Co–C bond is 1.95 Å, slightly longer than that of CoC_2H_2^- . The two Co–H bond lengths are calculated to be 1.63 and 1.75 Å, respectively. Isomer 2b is a structure consisting of two Co atoms inserted into two C–H bonds of acetylene. The calculated C–C bond length of isomer 2b is about 1.26 Å, which is longer than that of free acetylene (1.20 Å) and shorter than that of free ethene (1.33 Å). Isomer 2c is similar to isomer 2a except that isomer 2a is in the $^6A'$ electronic state while isomer 2c is in the $^4A''$ electronic state. The two Co–H bond lengths of isomer 2c are both calculated to be 1.66 Å. The theoretical VDEs of isomers 2a, 2b, and 2c are 1.80, 3.41, and 1.53 eV, respectively. Isomer 2d has a structure with a Co_2 dimer inserted into the C–H bond of acetylene. It is higher in energy than isomer 2a by 0.28 eV, and its VDE is calculated to be 2.53 eV.

Isomer 3a is the most stable structure of $\text{Co}_3\text{C}_2\text{H}_2^-$. It is composed of a five-member ring of Co_3C_2 carbide adsorbing two hydrogen atoms on its two Co–Co bonds. Isomer 3b is 0.10 eV higher in energy than isomer 3a. It consists of a five-member ring of Co_3C_2 carbide adsorbing two hydrogen atoms on its two nonadjacent Co vertices.⁴¹ Isomers 3c and 3d are energetically 0.33 and 0.34 eV above isomer 3a. They are composed of the five-member ring of the $\text{Co}_3\text{C}_2\text{H}$ cluster adsorbing a hydrogen atom on its different Co–Co bonds.⁴⁰ The calculated VDEs of isomers 3a–3d are 2.34, 3.10, 1.42, and 1.69 eV, respectively. The calculated C–C bond lengths of isomers 3a–3d are all 1.27 Å. They are longer than that of free acetylene (1.20 Å) and shorter than that of free ethene (1.33 Å).

B. Neutral $\text{Co}_n\text{C}_2\text{H}_2$ ($n = 1\text{--}3$) Clusters. The lowest-energy isomer of neutral CoC_2H_2 (1A) is a slightly bent structure with the 4A electronic ground state. The $\angle\text{CCoH}$ bond angle of isomer 1A is 153.8°, and the CoC_2H unit is almost linear. The Co–H and Co–C bond lengths are calculated to be 1.57 and 1.93 Å, respectively, similar to those of its anionic counterpart. The calculated C–C bond length is about 1.22 Å, also close to that of its anionic species as well as that of free acetylene. The calculated C–H, Co–C, and Co–H stretching vibrations of isomer 1A are 3447.8, 470.2, and 1852.3 cm^{-1} , respectively. The C–C stretching mode is calculated to be 2040.5 cm^{-1} , close to that of free acetylene (2061.2 cm^{-1}) and much higher than that of free ethene (1683.8 cm^{-1}) calculated at the same theoretical level, suggesting a $\text{C}\equiv\text{C}$ triple bond character in HCoC_2H (isomer 1A). Isomer 1B with the 2B_1 electronic state is 0.13 eV higher in energy than isomer 1A with the 4A electronic state. It is a side-on complex $\text{Co-}\eta^2\text{-(C}_2\text{H}_2)$. The C–C bond length is calculated to be 1.30 Å, close to that of free ethene (1.33 Å), indicating that the Co atom reduces the triple bond to a double bond. The Co–C bond lengths of isomer 1B are both 1.83 Å at the B3LYP level. Isomer 1C is 0.24 eV higher in energy than isomer 1A. It possesses a vinylidene structure with C_s symmetry and the $^2A''$ electronic state. The C–C bond length of isomer 1C is 1.31 Å at the B3LYP level, close to that of free ethene (1.33 Å). The Co–C bond length of isomer 1C is calculated to be ~ 1.74 Å, shorter than the Co–C covalent bond (1.83 Å); therefore, it may be a double bond.

The lowest-energy structure of the neutral $\text{Co}_2\text{C}_2\text{H}_2$ is isomer 2A. It is formed by adsorbing a hydrogen atom on the Co–Co bond of the $\text{Co}_2\text{C}_2\text{H}$ cluster, which has a similar structure with its corresponding anionic cluster. The C–C

bond length of isomer 2A is calculated to be 1.22 Å, very close to that of free acetylene (1.20 Å). Isomer 2B is 0.38 eV higher in energy than isomer 2A. It is formed by attaching a Co atom to the $\text{Co}=\text{C}=\text{CH}_2$ (isomer 1C) through a Co–Co bond. Isomer 2C is 0.71 eV higher in energy than isomer 2A. The geometry of isomer 2C is similar to that of isomer 2A. They are spinomers with the $^5\text{A}'$ electronic state for isomer 2A and the $^7\text{A}'$ electronic state for isomer 2C.

For the neutral $\text{Co}_3\text{C}_2\text{H}_2$ cluster, two almost energetically degenerate isomers (3A and 3B) with only a 0.02 eV energy difference are found. They are made up of a five-member ring of the $\text{Co}_3\text{C}_2\text{H}$ cluster adsorbing a hydrogen atom on its different Co–Co bonds.³⁷ The calculated C–C bond lengths of isomers 3A and 3B are 1.25 and 1.26 Å, respectively. Isomer 3C is 0.14 eV higher in energy than isomer 3A. Isomer 3C with the ^6A electronic state has a similar structure as isomer 3A in the ^8A electronic state. They are spinomers.

Figures 2 and 3 show that the geometries of the neutral $\text{Co}_n\text{C}_2\text{H}_2$ ($n = 1-2$) are similar to those of their anionic counterparts, whereas that of the neutral $\text{Co}_3\text{C}_2\text{H}_2$ is very different from its anionic counterpart. The geometries of anionic $\text{Co}_n\text{C}_2\text{H}_2^-$ ($n = 1-2$) and neutral $\text{Co}_n\text{C}_2\text{H}_2$ ($n = 1-3$) are made up of $\text{Co}_n\text{C}_2\text{H}$ adsorbing a hydrogen atom on the top or bridge sites of Co_n ($n = 1-3$). The geometry of anionic $\text{Co}_3\text{C}_2\text{H}_2^-$ is formed by a five-member ring of the anionic Co_3C_2 cluster adsorbing two hydrogen atoms on its two Co–Co bonds. The bare cobalt is an excellent magnetic material. In order to study the influence of acetylene on the magnetic moments of cobalt clusters, we calculated the magnetic moments of $\text{Co}_n\text{C}_2\text{H}_2$ ($n = 1-3$) clusters. The most preferred spin multiplicities of neutral $\text{Co}_n\text{C}_2\text{H}_2$ ($n = 1-3$) are the quartet, quintet, and octet, respectively. Hence, their most preferred magnetic moments are 3, 4, and $7 \mu_B$, respectively. These are the same as those of bare Co_n ($n = 1-3$).

It is worth noting that $\text{Co}_n\text{C}_2\text{H}_2$ clusters have some similarities and differences with $\text{Co}_n\text{C}_2\text{H}$ and Co_nC_2 ($n = 1-3$) clusters, which have been previously studied by anion photoelectron spectroscopy and DFT calculations.^{40,41} The geometries of anionic and neutral $\text{Co}_n\text{C}_2\text{H}_2$ are similar to those of $\text{Co}_n\text{C}_2\text{H}$ ($n = 1-3$) except for anionic $\text{Co}_3\text{C}_2\text{H}_2^-$, which is similar to the structure of anionic Co_3C_2 . The geometries of anionic and neutral $\text{Co}_n\text{C}_2\text{H}_2$, $\text{Co}_n\text{C}_2\text{H}$, and Co_nC_2 ($n = 1-3$) clusters are all planar or quasi-planar except for neutral Co_3C_2 , which is a three-dimensional structure. The characteristics of the C–C bonds in $\text{Co}_n\text{C}_2\text{H}_2$ ($n = 1-3$) are similar to those of the $\text{Co}_n\text{C}_2\text{H}$, while they are different from those of the Co_nC_2 ($n = 1-3$) clusters. The C–C bond lengths of $\text{Co}_n\text{C}_2\text{H}_2$ and $\text{Co}_n\text{C}_2\text{H}$ ($n = 1-3$) are much closer to the $\text{C}\equiv\text{C}$ bond length of free acetylene, whereas those of the Co_nC_2 ($n = 1-3$) clusters are much closer to the $\text{C}=\text{C}$ bond length of free ethene. The magnetic moments of the $\text{Co}_n\text{C}_2\text{H}_2$, $\text{Co}_n\text{C}_2\text{H}$, and Co_nC_2 ($n = 1-3$) clusters are all similar to those of bare Co_n ($n = 1-3$) clusters. The calculated VDEs of anionic $\text{Co}_n\text{C}_2\text{H}_2^-$ clusters ($n = 1-3$) are all higher than those calculated for the corresponding anionic $\text{Co}_n\text{C}_2\text{H}^-$ and Co_nC_2^- ($n = 1-3$) clusters.

C. Conversion Mechanisms among Isomers of the Neutral CoC_2H_2 Cluster. We investigated the conversion mechanisms of the inserted isomer HCoC_2H , the side-on complex $\text{Co}-\eta^2-(\text{C}_2\text{H}_2)$, and the vinylidene isomer $\text{Co}=\text{C}=\text{CH}_2$ for the neutral CoC_2H_2 cluster in doublet and quartet multiplicities. The optimized transition-state structures and isomers of the CoC_2H_2 cluster as well as their potential energy

diagrams are shown in Figure 4. The electronic states of isomers A–G are ^4A , $^2\text{B}_1$, $^2\text{A}''$, $^4\text{A}''$, ^2A , $^4\Sigma$, and $^4\text{A}''$, respectively.

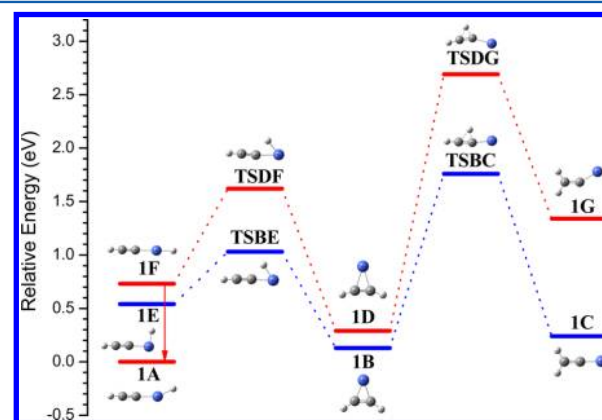


Figure 4. Potential energy profiles of the conversion mechanisms for isomers of the neutral CoC_2H_2 cluster in doublet and quartet multiplicities. The electronic states of isomers A–G are ^4A , $^2\text{B}_1$, $^2\text{A}''$, $^4\text{A}''$, ^2A , $^4\Sigma$, and $^4\text{A}''$, respectively.

In the quartet multiplicity, isomers 1F, 1D, and 1G can convert into each other through transition states TSDG and TSDG. The imaginary frequencies of the transition states TSDG and TSDG are -1281.3 and -1248.2 cm^{-1} , respectively. The transition-state structure TSDG was found to be 0.89 eV higher in energy than isomer 1F. Isomer 1F with the $^4\Sigma$ state can either relax to isomer 1A with the ^4A state spontaneously or convert into isomer 1D with the $^4\text{A}''$ state via TSDG. The reaction from isomer 1F to isomer 1D is exothermic by 0.44 eV and is a 1,2-hydrogen shift process from cobalt to carbon. The activation barrier of isomer 1D to 1G is 2.40 eV, much higher than that from 1F to 1D. Therefore, the conversion from isomer 1D to 1G is the rate-limiting step for the reaction of the inserted isomer into the vinylidene isomer. The reaction from isomer 1D to isomer 1G is endothermic by 1.05 eV and is a 1,2-hydrogen shift process between two carbons. In view of the reaction mechanisms and relative energies of isomers 1A (^4A), 1D ($^4\text{A}''$), 1F ($^4\Sigma$), and 1G ($^4\text{A}''$), it can be seen that isomer 1A with the ^4A state is favorable both kinetically and thermodynamically. In the doublet multiplicity, isomers 1B, 1C, and 1E can convert into each other through the transition states TSBE and TSBC. The imaginary frequencies of TSBE and TSBC are -704 and -1121.7 cm^{-1} . The transition-state structure TSBE is 0.49 eV higher than isomer 1E. The conversion from isomer 1E to 1B is exothermic by 0.41 eV and is a 1,2-shift process from cobalt to carbon. Isomer 1B can convert into isomer 1C through the transition state TSBC, which is 1.63 eV higher in energy than isomer 1B. It is much higher than the activation energy of isomer 1E to 1B; therefore, it is the rate-limiting step. On the basis of the reaction mechanisms and relative energies of isomers 1B, 1C, and 1E, it is obvious that isomer 1B is favorable both kinetically and thermodynamically. The pathways for the two multiplicities are both from the insertion isomer to the vinylidene isomer. It is an endothermic reaction in the quartet, while it is exothermic in the doublet. Moreover, the activation energies of the rate-limiting step are both the second step of the side-on complex converting into the vinylidene complex in the quartet and doublet multiplicities. As a whole, the reaction potential energy diagrams show that the inserted isomer HCoC_2H can convert

into the vinylidene complex $\text{Co}=\text{C}=\text{CH}_2$ by passing a side-on isomer $M-\eta^2-(\text{C}_2\text{H}_2)$.

5. CONCLUSIONS

We investigated anionic and neutral $\text{Co}_n(\text{C}_2\text{H}_2)$ ($n = 1-3$) clusters using DFT calculations as well as the CoC_2H_2^- by anion photoelectron spectroscopy. The ADE of CoC_2H_2^- is determined to be 1.82 eV from the experiment, and those of $\text{Co}_n\text{C}_2\text{H}_2^-$ ($n = 2-3$) are calculated to be 1.57 and 2.27 eV, respectively. On the basis of experimental and theoretical results, we found that the most stable geometries of anionic and neutral $\text{Co}_n\text{C}_2\text{H}_2$ ($n = 1-3$) are composed of $\text{Co}_n\text{C}_2\text{H}$ clusters adsorbing a hydrogen atom on the top or bridge sites of Co_n clusters except the anionic $\text{Co}_3\text{C}_2\text{H}_2^-$, which consists of a five-member ring of Co_3C_2 carbide adsorbing two hydrogen atoms on two bridge sites of Co_3 .

■ ASSOCIATED CONTENT

Supporting Information

Tables S1 and S2, showing the VDE of CoC_2H_2^- from the different functionals and the relative energies, VDEs, and C–C bond lengths for isomers of CoC_2H_2^- along with full ref 37. This material is available free of charge via the Internet at <http://pubs.acs.org>.

■ AUTHOR INFORMATION

Corresponding Author

*E-mail: zhengwj@iccas.ac.cn.

Notes

The authors declare no competing financial interest.

■ ACKNOWLEDGMENTS

This work was supported by the Natural Science Foundation of Education Department of Henan Province (No. 13B150987), the Natural Science Foundation of Zhengzhou City (No. 20120324), and the Natural Science Foundation of China (Grant No. 21273246). The theoretical calculations were conducted on ScGrid and DeepComp 7000 at the Supercomputing Center, the Computer Network Information Center of the Chinese Academy of Sciences.

■ REFERENCES

- (1) Wang, X.; Andrews, L. Infrared Spectra of Rh Atom Reaction Products with C_2H_2 : The HRhCCh , RhCCh , RhCCH_2 , and $\text{Rh}-\eta^2-\text{C}_2\text{H}_2$ Molecules. *J. Phys. Chem. A* **2011**, *115*, 9447–9455.
- (2) Kline, E. S.; Kafafi, Z. H.; Hauge, R. H.; Margrave, J. L. FTIR Matrix Isolation Studies of the Reactions of Atomic and Diatomic Nickel with Acetylene in Solid Argon. The Photosynthesis of Nickel Vinylidene. *J. Am. Chem. Soc.* **1987**, *109*, 2402–2409.
- (3) Kasai, P. H. Aluminum Atom–Ethylene and Aluminum Atom–Acetylene Complexes: Matrix Isolation Electron Spin Resonance Study. *J. Am. Chem. Soc.* **1982**, *104*, 1165–1172.
- (4) Lee, Y. K.; Manceron, L.; Papai, I. An IR Matrix Isolation and DFT Theoretical Study of the First Steps of the $\text{Ti}(0)$ Ethylene Reaction: Vinyl Titanium Hydride and Titanacyclopentene. *J. Phys. Chem. A* **1997**, *101*, 9650–9659.
- (5) Teng, Y.-L.; Xu, Q. Matrix Isolation Infrared Spectroscopic and Density Functional Theoretical Studies on the Reactions of Lanthanum Atoms with Acetylene. *J. Phys. Chem. A* **2008**, *112*, 10274–10279.
- (6) Kline, E. S.; Kafafi, Z. H.; Hauge, R. H.; Margrave, J. L. Matrix-Isolation Studies of the Reactions of Iron Atoms and Iron Dimers with Acetylene in an Argon Matrix. The FT-IR Spectrum of Ethynyliron Hydride. *J. Am. Chem. Soc.* **1985**, *107*, 7559–7562.

(7) Teng, Y.-L.; Xu, Q. Reactions of Yttrium and Scandium Atoms with Acetylene: A Matrix Isolation Infrared Spectroscopic and Theoretical Study. *J. Phys. Chem. A* **2010**, *114*, 9069–9073.

(8) Chenier, J. H. B.; Howard, J. A.; Mile, B.; Sutcliffe, R. Cryochemical Studies. 3. ESR Studies of the Reaction of Group IB Metal Atoms with Acetylene and Phenylacetylene in a Rotating Cryostat. *J. Am. Chem. Soc.* **1983**, *105*, 788–791.

(9) Huang, Z.; Zeng, A.; Dong, J.; Zhou, M. Matrix Isolation Fourier Transform Infrared Spectroscopic and Density Functional Theoretical Studies of the Reactions of Chromium Atoms and Acetylene. *J. Phys. Chem. A* **2003**, *107*, 2329–2333.

(10) Wang, X.; Andrews, L. Infrared Spectra and Density Functional Calculations for Three $\text{Pt}-\text{C}_2\text{H}_2$ Reaction Product Isomers: PtCCH_2 , HPtCCH , and $\text{Pt}-\eta^2-(\text{C}_2\text{H}_2)$. *J. Phys. Chem. A* **2004**, *108*, 4838–4845.

(11) Wang, X.; Andrews, L. Side-Bonded $\text{Pd}-\eta^2-(\text{C}_2\text{H}_2)_{1,2}$ and $\text{Pd}_3-\eta^2-(\text{C}_2\text{H}_2)$ Complexes: Infrared Spectra and Density Functional Calculations. *J. Phys. Chem. A* **2002**, *107*, 337–345.

(12) Andrew, L.; Kushto, G. P.; Marsden, C. J. Reactions of Th and U Atoms with C_2H_2 : Infrared Spectra and Relativistic Calculations of the Metallacyclopentene, Actinide Insertion, and Ethynyl Products. *Chem.—Eur. J.* **2006**, *12*, 8324.

(13) Cho, H.-G.; Andrews, L. Infrared Spectra of $M-\eta^2-\text{C}_2\text{H}_2$, $\text{HM}-\text{C}\equiv\text{CH}$, and $\text{HMC}\equiv\text{CH}^-$ Prepared in Reactions of Laser-Ablated Group 3 Metal Atoms with Acetylene. *J. Phys. Chem. A* **2012**, *116*, 10917–10926.

(14) Wang, Q.; Wang, X.; Andrews, L. The HRuCCH , RuCCH_2 , and $\text{Ru}-\eta^2-\text{C}_2\text{H}_2$ Molecules: Infrared Spectra and Density Functional Calculations. *J. Phys. Chem. A* **2011**, *115*, 12194–12200.

(15) Cho, H.-G.; Andrews, L. Infrared Spectra of the Ethynyl Metal Hydrides Produced in Reactions of Laser-Ablated Mn and Re Atoms with Acetylene. *J. Phys. Chem. A* **2011**, *115*, 4929–4934.

(16) Cho, H.-G.; Lyon, J. T.; Andrews, L. Infrared Spectra of $M-\eta^2-\text{C}_2\text{H}_2$ and $\text{HM}-\text{C}\equiv\text{CH}$ Produced in Reactions of Laser-Ablated Group 6 Metal Atoms with Acetylene. *J. Phys. Chem. A* **2012**, *116*, 11880–11887.

(17) Teng, Y.-L.; Xu, Q. Reactions of Group 14 Metal Atoms with Acetylene: A Matrix Isolation Infrared Spectroscopic and Theoretical Study. *J. Phys. Chem. A* **2009**, *113*, 12163–12170.

(18) France, M. R.; Pullins, S. H.; Duncan, M. A. Photodissociation Spectroscopy of the $\text{Ca}^+-\text{C}_2\text{H}_2$ and $\text{Ca}^+-\text{C}_2\text{D}_2$ π Complexes. *J. Chem. Phys.* **1998**, *109*, 8842–8850.

(19) Walters, R. S.; Jaeger, T. D.; Duncan, M. A. Infrared Spectroscopy of $\text{Ni}^+(\text{C}_2\text{H}_2)_n$ Complexes: Evidence for Intracuster Cyclization Reactions. *J. Phys. Chem. A* **2002**, *106*, 10482–10487.

(20) Walters, R. S.; Pillai, E. D.; Schleyer, P. v. R.; Duncan, M. A. Vibrational Spectroscopy and Structures of $\text{Ni}^+(\text{C}_2\text{H}_2)_n$ ($n = 1-4$) Complexes. *J. Am. Chem. Soc.* **2005**, *127*, 17030–17042.

(21) Walters, R. S.; Schleyer, P. v. R.; Corminboeuf, C.; Duncan, M. A. Structural Trends in Transition Metal Cation–Acetylene Complexes Revealed through the C–H Stretching Fundamentals. *J. Am. Chem. Soc.* **2005**, *127*, 1100–1101.

(22) Ramsvik, T.; Borg, A.; Venvik, H. J.; Hansteen, F.; Kildemo, M.; Worren, T. Acetylene Chemisorption and Decomposition on the $\text{Co}(1120)$ Single Crystal Surface. *Surf. Sci.* **2002**, *499*, 183–192.

(23) Khodakov, A. Y.; Chu, W.; Fongarland, P. Advances in the Development of Novel Cobalt Fischer–Tropsch Catalysts for Synthesis of Long-Chain Hydrocarbons and Clean Fuels. *Chem. Rev.* **2007**, *107*, 1692–1744.

(24) Song, W.; Ackermann, L. Cobalt-Catalyzed Direct Arylation and Benzoylation by C–H/C–O Cleavage with Sulfamates, Carbamates, and Phosphates. *Angew. Chem., Int. Ed.* **2012**, *51*, 8251–8254.

(25) Punji, B.; Song, W.; Shevchenko, G. A.; Ackermann, L. Cobalt-Catalyzed C–H Bond Functionalizations with Aryl and Alkyl Chlorides. *Chem.—Eur. J.* **2013**, *19*, 10605–10610.

(26) Xu, H.-G.; Zhang, Z.-G.; Feng, Y.; Yuan, J. Y.; Zhao, Y. C.; Zheng, W. J. Vanadium-Doped Small Silicon Clusters: Photoelectron Spectroscopy and Density-Functional Calculations. *Chem. Phys. Lett.* **2010**, *487*, 204–208.

(27) Stephens, P. J.; Devlin, F. J.; Chabalowski, C. F.; Frisch, M. J. Ab Initio Calculation of Vibrational Absorption and Circular Dichroism Spectra Using Density Functional Force Fields. *J. Phys. Chem.* **1994**, *98*, 11623–11627.

(28) Becke, A. D. Density-Functional Exchange-Energy Approximation with Correct Asymptotic Behavior. *Phys. Rev. A* **1988**, *38*, 3098–3100.

(29) Becke, A. D. Density-Functional Thermochemistry. III. The Role of Exact Exchange. *J. Chem. Phys.* **1993**, *98*, 5648–5652.

(30) Lee, C.; Yang, W.; Parr, R. G. Development of the Colle–Salvetti Correlation-Energy Formula into a Functional of the Electron Density. *Phys. Rev. B* **1988**, *37*, 785–789.

(31) Cho, H.-G.; Kushto, G. P.; Andrews, L.; Bauschlicher, C. W. Infrared Spectra of $\text{HC}\equiv\text{CMH}$ and $M\text{-}\eta^2\text{-(C}_2\text{H}_2)$ from Reactions of Laser-Ablated Group-4 Transition-Metal Atoms with Acetylene. *J. Phys. Chem. A* **2008**, *112*, 6295–6304.

(32) Barden, C. J.; Rienstra-Kiracofe, J. C.; Schaefer, H. F., III. Homonuclear 3d Transition-Metal Diatomics: A Systematic Density Functional Theory Study. *J. Chem. Phys.* **2000**, *113*, 690–700.

(33) Gutsev, G. L.; Bauschlicher, C. W., Jr. Chemical Bonding, Electron Affinity, and Ionization Energies of the Homonuclear 3d Metal Dimers. *J. Phys. Chem. A* **2003**, *107*, 4755–4767.

(34) Cramer, C. J.; Truhlar, D. G. Density Functional Theory for Transition Metals and Transition Metal Chemistry. *Phys. Chem. Chem. Phys.* **2009**, *11*, 10757–10816.

(35) Gonzalez, C.; Schlegel, H. B. Reaction Path Following in Mass-Weighted Internal Coordinates. *J. Phys. Chem.* **1990**, *94*, 5523–5527.

(36) Boys, S. F.; Bernardi, F. The Calculation of Small Molecular Interactions by the Differences of Separate Total Energies. Some Procedures with Reduced Errors. *Mol. Phys.* **1970**, *19*, 553.

(37) Frisch, M. J.; Trucks, G. W.; Schlegel, H. B.; Scuseria, G. E.; Robb, M. A.; Cheeseman, J. R.; Zakrzewski, V. G.; Montgomery, J. A., Jr.; Stratmann, R. E.; Burant, J. C.; et al. *Gaussian 03*; Gaussian, Inc.: Wallingford, CT, 2004.

(38) Dean, J. A. *Properties of Atoms, Radicals, and Bonds. Lange's Handbook of Chemistry*, 15th ed.; McGraw-Hill Press: New York, 1999; Section 4, p 36.

(39) Dean, J. A. *Properties of Atoms, Radicals, and Bonds. Lange's Handbook of Chemistry*, 15th ed.; McGraw-Hill Press: New York, 1999; Section 4, p 38.

(40) Yuan, J.-Y.; Xu, H.-G.; Zhang, Z.-G.; Feng, Y.; Zheng, W.-J. Adsorption of C_2H Radical on Cobalt Clusters: Anion Photoelectron Spectroscopy and Density Functional Calculations. *J. Phys. Chem. A* **2011**, *115*, 182–186.

(41) Yuan, J.-Y.; Xu, H.-G.; Zheng, W.-J. Photoelectron Spectroscopy and Density Functional Study of Co_nC_2^- ($n = 1\text{--}5$) Clusters. *Phys. Chem. Chem. Phys.* **2014**, *16*, 5434–5439.